Analyst

PAPER

View Article Online
View Journal | View Issue

Cite this: *Analyst*, 2020, **145**, 6262

Colorimetric detection of Hg^{2+} with an azulene-containing chemodosimeter *via* dithioacetal hydrolysis†

Carlos M. López-Alled, [a] Lloyd C. Murfin, [b] Gabriele Kociok-Köhn, [c] Tony D. James, *[a,b] Jannis Wenk *[a,d] and Simon E. Lewis *[a,b]

Received 14th July 2020,
Accepted 4th September 2020

DOI: 10.1039/d0an01404d

rsc.li/analyst

Azulene is a bicyclic aromatic chromophore that absorbs in the visible region. Its absorption maximum undergoes a hypsochromic shift if a conjugated electron-withdrawing group is introduced at the C1 position. This fact can be exploited in the design of a colorimetric chemodosimeter that functions by the transformation of a dithioacetal to the corresponding aldehyde upon exposure to Hg^{2+} ions. This chemodosimeter exhibits good chemoselectivity over other metal cations, and responds with an unambiguous colour change clearly visible to the naked eye. Its synthesis is concise and its ease of use makes it appropriate in resource-constrained environments, for example in determing mercury content of drinking water sources in the developing world.

Introduction

Mercury (elemental symbol Hg; atomic number 80; atomic weight 200.592 g mol^{-1}; aqueous solubility at 25 °C = 2.8 × 10^{-7} mol L^{-1}) is a silvery-white group 12 metal, which is liquid at room temperature.[1–3] Mercury has the oxidation states +I and +II and is ubiquitous in the environment, where it exists as elemental, inorganic and organic mercury species. The average mercury content of the earth's crust is 0.05 mg kg^{-1}.[4] Mercury occurs in rocks, usually below 0.02 mg kg^{-1} but at higher concentration in mercury minerals and organic sedimentary deposits. Usually, mercury can be found in most uncontaminated soils at concentration below 1 mg kg^{-1}, in rivers (1–5 ng L^{-1}), lakes (0.2–80 ng L^{-1}), groundwater (0.1–16 ng L^{-1}), rainwater (5.0–90 ng L^{-1}), ocean water (0.2–4 ng L^{-1})[5] and in the atmosphere (0.8–1.8 ng m^{-3}).[6] Biogeochemical transport processes including transformation mechanisms of mercury species are complex, while natural mercury fluxes and its occurrence in the environment have been altered by human activities.[7] Mercury is toxic to humans, animals, plants and microorganisms.[8] The World Health Organization (WHO) provides information documents on the most prevalent pathways of human exposure to mercury.[9] Governments and intergovernmental bodies such as the European Commission set the maximum levels for mercury in food and water.[10] The drinking water standard for mercury is 1 μg L^{-1} in Europe[11] and 2 μg L^{-1} in the US,[12] respectively. Due to mercury's harmful effects on human health and ecosystems, the use of many products containing mercury has been phased out. Reduction of anthropogenic mercury emissions is an objective in most of the international efforts towards a sustainable economy, such as the Minamata, Rotterdam and Basel conventions.[13–17]

Anthropogenic mercury emissions will depend on future patterns of fossil fuel usage, on uptake of mercury removal technologies[18] and on continuing implementation of mercury reduction policies.[7a] However, more mercury pollution is caused by artisanal and small-scale gold mining (ASGM) than any other human activity. In ASGM, elemental mercury is used as a lixiviant (solubilising recovery agent) for gold ore,[19] forming an amalgam that is then heated to distil off the mercury and recover the gold. ASGM is an unregulated activity and typically no attempt is made to recover the mercury in this step. This leads to high concentrations of mercury(0) in the local environment with consequent severe adverse health effects for local residents, including neurological and kidney damage.[20] Mercury passes into water by diffusion, and is oxidised to Hg(II) by various bioprocesses.[21] Additionally, in many regions, miners can transfer the tailings (residues) from their activities to larger processing centres, which then use cyanide leaching techniques to extract additional gold. The combi-

[a]*Centre for Sustainable and Circular Technologies, University of Bath, Bath, BA2 7AY, UK. E-mail: T.D.James@bath.ac.uk, J.H.Wenk@bath.ac.uk, S.E.Lewis@bath.ac.uk*
[b]*Department of Chemistry, University of Bath, Bath, BA2 7AY, UK*
[c]*Materials and Chemical Characterization (MC²), University of Bath, Bath, BA2 7AY, UK*
[d]*Department of Chemical Engineering & Water Innovation & Research Centre: WIRC @ Bath, University of Bath, Bath, BA2 7AY, UK*

†Electronic supplementary information (ESI) available: Experimental procedures. Characterisation data for **3**. See DOI: 10.1039/d0an01404d

nation of mercury residues in the tailings with cyanide leads to the formation of soluble complexes such as $Hg(CN)_2$ or $[Hg(CN)_4]^{2-}$ which may then be discharged directly to local water systems.[22] Constant monitoring of mercury in the wastewater of these facilities is essential to reduce the environmental impact and improve the sustainability of this sector. In comparison to the inorganic Hg(II) species described above, which are formed comparatively rapidly, formation of organic mercury species (primarily methylmercury) occurs in microbiological soil and sediment processes that operate on a longer timescale.[5a] Thus, detection of inorganic Hg(II) is the most appropriate strategy for surveillance of unimproved drinking water in communities affected by ASGM.

In view of the above, there is a significant impetus to develop methods to quantify mercury in water, both in watercourses in affected communities and in polluting industries. Established analytical methods to determine total mercury and its speciation include inductively coupled mass or atomic spectrometry and gas chromatography,[23–27] as well as fluorescence titration.[28] However, these techniques require a laboratory setting and expert personnel. An ideal method of quantitation of mercury for use in the field would function without recourse to specialised equipment, a power supply, or highly trained users. In this context, a naked-eye colorimetric assay would be ideal, as such assays have none of the above requirements, and could be performed by residents of the affected communities. Furthermore, such a test does not require the user to be literate.

Numerous colorimetric assays for Hg^{2+} have been reported,[29] and they may be divided into those that involve the reversible coordination of mercury to a molecular receptor (chemical sensors)[30] and those that function by an irreversible mercury-induced chemical reaction (chemodosimeters). Designs for mercury chemodosimeters have been reported that exploit several different mercury-induced transformations, such as hydrolysis of thiocarbonyl functional groups to the corresponding carbonyls, or mercury-induced heterocycle formation.[31] We opted to employ the mercury-mediated hydrolysis of a dithioacetal, a transformation that was first reported in the field of organic synthesis, where it enables so-called "umpolung" carbonyl reactivity. Its use in a mercury chemodosimeter has precedent, with the first report in 2009 from Kim and Kim describing a dithiane-appended coumarin, which changed from colourless to yellow upon exposure to Hg^{2+} and also exhibited a fluorescence response.[32] Many subsequent reports of mercury chemodosimeters based on dithiane hydrolysis have been published, although most of these concern fluorescent probes.[33–35] Far less common are *colorimetric* probes based on dithiane hydrolysis; of these, most reports describe fluorescent probes which have been noted also to exhibit a colour change.[33f,g,l,n,t,v,w,y,34a,b,l,r,v,x,35a] To our knowledge there are only two prior reports of dithiane probes whose response is solely colorimetric. Li, Li and co-workers described a dithiane azo dye which exhibited a yellow-to-red response to Hg^{2+} in MeCN.[36] Li and co-workers later also reported a triarylamine-dithiane-nitroaryl dosimeter, which upon exposure to Hg^{2+} and subsequently to base, gave a colourless-to-purple response in THF.[37] It should be noted that colorimetric assays for organic mercury species have also been reported.[38] These are conceptually distinct processes that operate through reactions of organic mercury at the surface of gold nanoparticles.

In this work, we describe a colorimetric chemodosimeter for Hg^{2+} that employs an azulene as the chromophore. Azulene, **1**, is a non-alternant, bicyclic aromatic compound comprising a five-membered and a seven-membered ring. Although it is an isomer of naphthalene, its properties are quite different. For example, although it is a hydrocarbon, it has a significant dipole (1.08 D). Furthermore, its non-alternant nature leads to a smaller HOMO–LUMO energy gap compared to naphthalene. This leads to a transition in the visible region, and hence azulene has a vivid blue colour.[39] It has been shown that introducing electron-donating or electron-withdrawing substituents onto the azulene core results in a change in colour, due to perturbation of the absorption spectrum. Systematic studies have determined trends relating the position of a substituent (and its electronic nature) to the resultant colour.[40] Thus, any particular colour desired may be accessed through a design strategy that exploits these trends. Azulene derivatives have been employed as colorimetric sensors for a variety of analytes.[41] There are reports of colorimetric azulene-containing Hg^{2+} *sensors* (*i.e.* species that coordinate Hg^{2+} reversibly to achieve a colorimetric response). Wakabayashi and co-workers reported an azulene derivative with thiazole substituents,[42a] as well as an azulene with thioether and 2-pyridyl substituents[42b] and a 1,3-bis(2-pyridyl) azulene.[42c] Razus, Birzan and co-workers reported azulenes bearing 2,6-bis(heteroaryl)-4-pyridyl groups.[43] Buica, Ungureanu and co-workers reported an EDTA-bis(azulene) sensor.[44] Also of note, Kubo, Mori and co-workers reported an azulene-appended dithiacrown ether as a Hg^{2+} chelator for use in liquid–liquid extraction.[45] However to our knowledge, there has been no previous report of a colorimetric azulene-containing Hg^{2+} *chemodosimeter* (*i.e.* an irreversible, reaction-based probe). In view of our continuing interest in stimuli-responsive azulenes,[46] we targeted the development of an azulene-dithiane colorimetric dosimeter for detection of Hg^{2+} ions, and we report our results here.

Results and discussion

Our design strategy for a Hg^{2+}-responsive azulene chemodosimeter utilises the known characteristic of azulene that the introduction of an electron-withdrawing group at the 1-position affords maroon/red-coloured compounds.[40] Thus, azulene **1** has its S_0–S_1 band centred at λ_{max} = 580 nm (in hexane), resulting in the absorption of green and red light; its blue colour arises as a result of a lack of absorption in the blue region. In contrast, azulene-1-carbaldehyde **2** has a lower-lying HOMO, resulting in a blueshift of the S_0–S_1 band (to λ_{max} = 542 nm in hexane), and hence the observed maroon/pink colour. We reasoned that dithiane **3** ought to exhibit an absorption spectrum much closer to that of **1** than **2**, since the

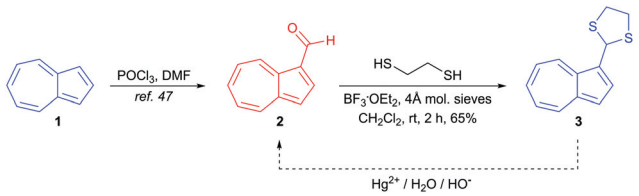

Scheme 1 Synthesis of colorimetric azulene mercury(II) chemodosimeter.

C1 substituent in **3** is an sp^3-hybridised carbon and hence the dithiane exerts no mesomeric effect on the azulene core. While sulfur is moderately electronegative, any electron-withdrawing effect will be lessened by distance. We therefore anticipated that **3** would have a blue colour. Synthesis of **3** was effected in one step from known aldehyde **2**,[47] as shown in Scheme 1.

Novel dithiane **3** was fully characterised by spectroscopic techniques including NMR, IR and MS. The identity of **3** was further confirmed through X-ray crystallography (Fig. 1). To the naked eye, **3** appeared blue in the solid state and in solution, with λ_{max} = 590 nm (H_2O/MeCN 8 : 2).

The colorimetric response of **3** to Hg^{2+} was assessed by preparing a solution of **3** and $Hg(NO_3)_2$ (H_2O/MeCN 8 : 2), and comparing this to a solution of **3** only. A distinct visible response was observed, but instead of the expected formation of the characteristic maroon/pink colour of **2**, a much more intense blue colour developed. A selectivity test was conducted, comparing the response of **3** to other metal cations (Fig. 2). It can be seen that Hg^{2+} induces the most pronounced increase in intensity of the blue colour, and less pronounced responses were observed for Ag^+ and (weakly) for Cu^{2+}.

The solution of **3** treated with $Hg(NO_3)_2$ exhibited significant absorption in the red region, with λ_{max} = 605 nm, hence the intense blue colour. The absorption spectrum of this solution exhibited maxima different from those of both **3** and **2**. Thus, while coordination between **3** and Hg^{2+} is undoubtedly occurring, the desired deprotection reaction is not. However, by modifying the conditions, we were able to induce the expected colour change to maroon/pink in the presence of Hg^{2+}. Specifically, $NaOH_{(aq)}$ was used (at a concentration of 10 mM), in addition to the other reaction components (there is precedent[48] in the synthetic literature for the addition of base to Hg^{2+}-mediated dithiane hydrolysis reactions in H_2O/MeCN). In view of this finding, we then sought evidence to confirm that the maroon/pink colour was indeed due to the regeneration of aldehyde **2** *in situ*. A comparison of the absorption spectrum of **2** with that of **3** + $Hg(NO_3)_2$ + NaOH showed their absorption maxima to be coincident (Fig. 3).

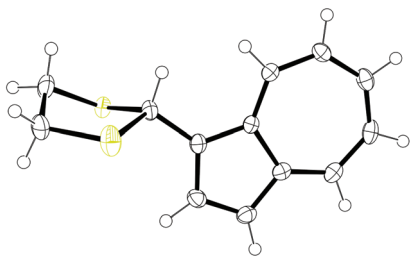

Fig. 1 Solid state structure of **3**, crystallised from CH_2Cl_2/petroleum ether. Ellipsoids are represented at 50% probability. H atoms are shown as spheres of arbitrary radius. CCDC 1958284.†

Fig. 2 Naked-eye selectivity experiment of **3** (500 μM) exposed to $Hg(NO_3)_2$, LiCl, NaCl, KCl, $Mg(NO_3)_2$, $CaCl_2$, $FeSO_4$, $Ni(acac)_2$, $CuCl_2$, $Zn(NO_3)_2$, $AgNO_3$, $Pb(OAc)_2$, $Cd(OAc)_2$ and $As(NO_3)_3$ (each at 500 μM). The data were obtained in MeCN/H_2O solutions (2 : 8, v/v) and the photos were taken 30 min after mixing of **3** and the metal salts.

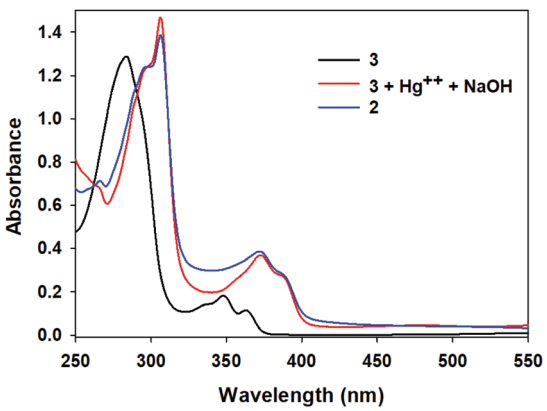

Fig. 3 UV-Vis spectra of **3** (180 μM); **3** (180 μM), $Hg(NO_3)_2$ (180 μM) and NaOH (10 mM); and **2** (180 μM). Spectra acquired 30 min after sample preparation (MeCN/H_2O, 2 : 8, v/v).

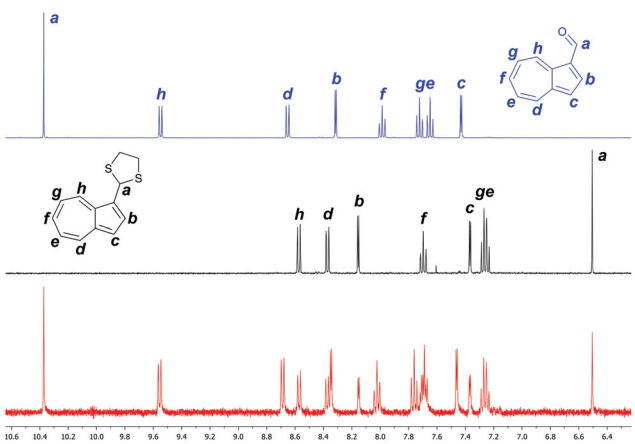

Fig. 4 ^{1}H-NMR spectra of **2** (top), **3** + NaOH (middle) and **3** + NaOH + 0.5 eq. $Hg(NO_3)_2$ (bottom). Spectra acquired in D_2O/CD_3CN.

An NMR study was carried out, comparing the ^{1}H spectra of **2**, **3** + NaOH, and **3** + NaOH + $Hg(NO_3)_2$. The spectrum of **2** contains azulenyl proton resonances in the range δ = 7.4–9.6 ppm, typical of an electron-poor azulene. The diagnostic aldehyde signal is clearly visible at δ = 10.37 ppm (Fig. 4, top). In the spectrum of **3**, the azulenyl signals are shifted upfield, and are observed in the range δ = 7.2–8.6 ppm, as the electron-withdrawing substituent is no longer present. The aldehyde peak is no longer observed, and instead the diagnostic dithiane methine signal is visible at δ = 6.50 ppm (Fig. 4, middle). The dithiane methylene signals are observed between δ = 3.43 and 3.65 ppm (not shown). The assignment of the peaks for **3** is based on interactions in the NOESY spectrum between H^a and H^h, and in the COSY spectrum between H^b–H^c and between H^d–H^e–H^f–H^g–H^h (see ESI†). In the spectrum of **3** treated with NaOH and with half an equivalent of $Hg(NO_3)_2$, resonances attributable to both **3** and **2** can be observed, both of them having approximately equal integrations. Most clearly, the aldehyde signal and the dithiane methine signal are both present. No signals from any other species are observed. These findings show that **2** is indeed formed from **3** upon exposure to Hg^{2+} under the conditions of the assay. Furthermore, they indicate a 1 : 1 reaction stoichiometry between Hg^{2+} ions and **3**, *i.e.* Hg^{2+} does not act as a catalyst in the transformation of **3** into **2**. This may be rationalised by the Hg^{2+} ion being sequestered in a chelate with the free ethane-1,2-dithiol after the

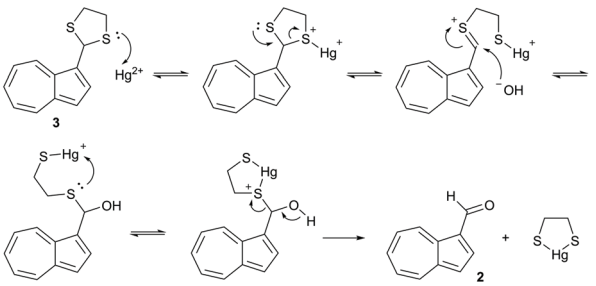

Scheme 2 Proposed mechanism of Hg^{2+} recognition.

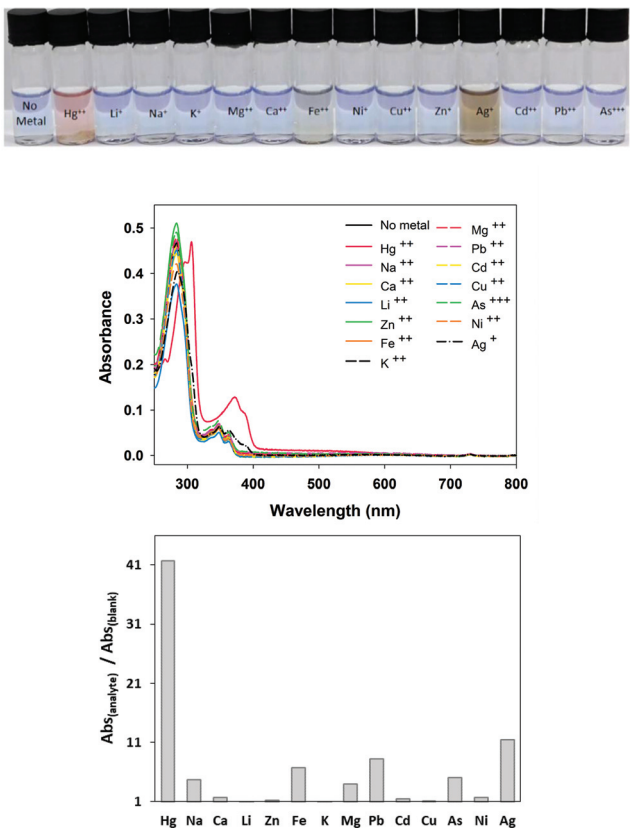

Fig. 5 Top. Naked-eye selectivity experiment of **3** (500 μM) and NaOH (10 mM), exposed to $Hg(NO_3)_2$, LiCl, NaCl, KCl, $Mg(NO_3)_2$, $CaCl_2$, $FeSO_4$, $Ni(acac)_2$, $CuCl_2$, $Zn(NO_3)_2$, $AgNO_3$, $Pb(OAc)_2$, $Cd(OAc)_2$ and $As(NO_3)_3$ (each at 500 μM). The data were obtained in $MeCN/H_2O$ solutions (2 : 8, v/v) and the photos were taken 30 min after. Middle. Absorption spectra of test solutions in the photo, diluted ten-fold. Bottom. Absorbance with the various metal ions at 307 nm.

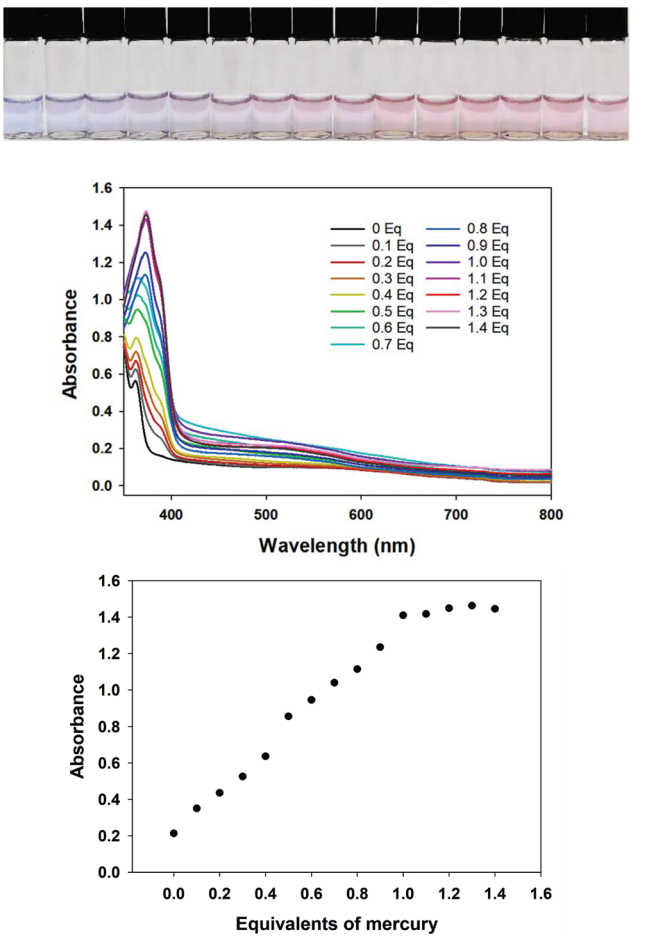

Fig. 6 Top. Naked-eye titration experiment of **3** (500 μM) and NaOH (10 mM) exposed to 50, 100, 150, 200, 250, 300, 350, 400, 450, 500, 550, 600, 650 and 700 μM of $Hg(NO_3)_2$. Photos were taken after 30 min in $MeCN/H_2O$ (2 : 8, v/v). Middle. Absorption spectra of test solutions in the photo, diluted ten-fold. Bottom. Dose–response curve, plotted using the absorbance values at 375 nm.

dithiane hydrolysis is complete, and hence being unable to react further (Scheme 2).

A subsequent selectivity test was conducted, comparing the response of **3** to other metal cations in the presence of NaOH to induce the dithiane cleavage (Fig. 5). It can be seen that only Hg^{2+} induces the characteristic colour change to maroon/pink. Responses were also observed for Ag^{+} and (weakly) for Fe^{2+}, albeit not forming the same maroon/pink colour. We propose that while some formation of **2** may be occurring with Ag^{+}, formation of silver oxide under the basic conditions is likely the main source of the response; in the context of mercury-contaminated watercourses, the co-occurrence of Ag^{+} is not expected.

Titration of **3** with Hg^{2+} in acetonitrile/water showed a linear response (r = 0.9963) between 0 and 1 equivalents of Hg^{2+}, above which saturation of the signal was observed (Fig. 6). This provides further confirmation of the 1 : 1 stoichiometry of the reaction between **3** and Hg^{2+}, in agreement with the findings of the NMR study (Fig. 4). The limit of detection of **3** towards Hg^{2+} was determined to be 1.65 mg L^{-1} (Fig. S1†). Evaluation of the fluorescence properties of **2** and **3** showed that both species were weakly emissive, and had emission maxima at similar wavelengths (Fig. S2†). These observations discouraged our evaluation of **3** as a fluorescent probe for Hg^{2+}.

While these results above vindicate our design strategy insofar as the chemodosimeter shows both good analyte selectivity and an unambiguous colour change, the requirement of using an organic co-solvent (acetonitrile) is less desirable for an in-the-field mercury test kit. In the initial evaluation of **3** described above, we adopted the use of the co-solvent out of necessity, as **3** itself is insoluble in pure water. However, we then explored the alternative approach of using a surfactant additive, in order to remove the need for an organic co-solvent. Brij™ C10 is a non-toxic, non-ionic surfactant that is known to be biodegradable.[49] When using 0.1% w/v of Brij™ C10 in water, **3** was effectively solubilised and showed a colorimetric response to Hg^{2+} ions. Furthermore, this response was as selective as when using the organic co-solvent, with confounding signals being observed only for Fe^{2+} and Ag^{+} ions (Fig. 7). Here again, we ascribe this to the formation of silver oxide.

Titration of **3** with Hg^{2+} in the water/Brij system (Fig. 8) showed a linear response once again (r = 0.9812), demonstrat-

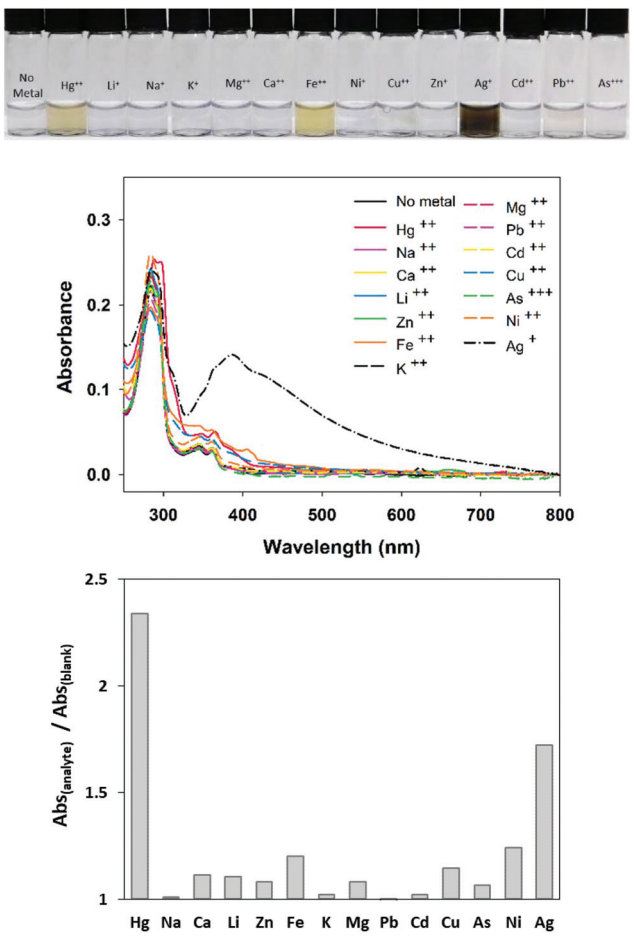

Fig. 7 Top. Naked-eye selectivity test of **3** (500 μM) and NaOH (10 mM) exposed to $Hg(NO_3)_2$, LiCl, NaCl, KCl, $Mg(NO_3)_2$, $CaCl_2$, $FeSO_4$, $Ni(acac)_2$, $CuCl_2$, $Zn(NO_3)_2$, $AgNO_3$, $Pb(OAc)_2$, $Cd(OAc)_2$ and $As(NO_3)_3$ (each at 500 μM). Photos were taken after 30 min water + 0.1% (w/v) Brij™ C10. Middle. Absorption spectra of test solutions in the photo, diluted tenfold. Bottom. Absorbance with the various metal ions at 300 nm.

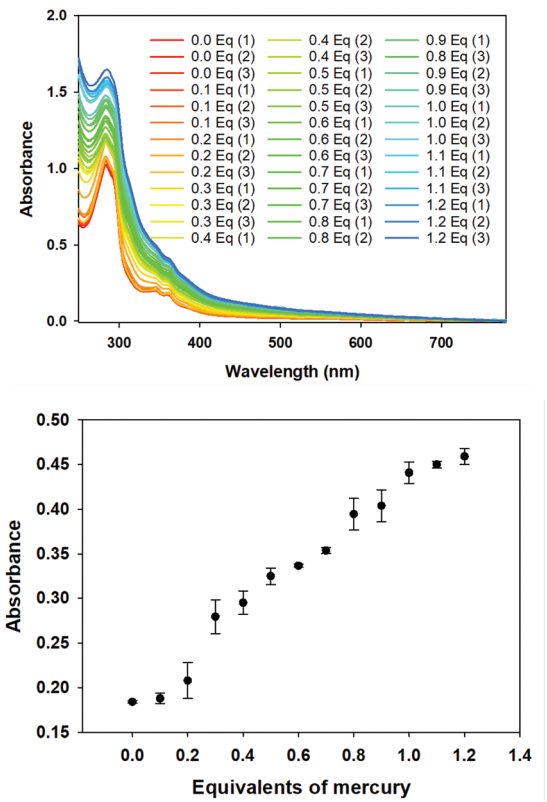

Fig. 8 Top. Absorption spectra of **3** (500 μM) and NaOH (10 mM) exposed to 50, 100, 150, 200, 250, 300, 350, 400, 450, 500, 550 and 600 μM of $Hg(NO_3)_2$. Spectra acquired after 30 min in water + 0.1% (w/v) Brij™ C10. Bottom. Dose–response curve, plotted using the absorbance values at 350 nm.

ing the viability of quantifying the concentration of mercury ions with this purely aqueous system.

Conclusions

We have synthesised and fully characterised a novel chemodosimeter **3** in two steps from azulene **1** and demonstrated its quantitative response to Hg^{2+} ions. Evidence for the regeneration of azulene aldehyde **2** under the assay conditions has been presented in the form of NMR and UV-vis absorbance spectroscopic data. Selectivity for Hg^{2+} over other metal cations has been determined. The assay procedure is operationally straightforward and furthermore can be carried out in the absence of an organic co-solvent if a surfactant is used. This system may therefore find applications in drinking water safety analysis in a developing world context.

Conflicts of interest

There are no conflicts to declare.

Acknowledgements

We are grateful for PhD funding to C.M.L.-A. from the EU Horizon 2020 research and innovation programme under grant agreement H2020-MSCA-CO-FUND, #665992. The British-Spanish Society and Plastic Energy are thanked for a 2017 Scholarship to C.M.L.-A. The EPSRC Impact Acceleration Account provided funding to L.C.M. under grant EP/R51164X/1. T.D.J. thanks the Royal Society for a Wolfson Merit Award. The Centre for Sustainable Circular Technologies is supported by EPSRC under grant EP/L016354/1.

Notes and references

1 *CRC handbook of chemistry and physics*, Taylor & Francis, Current internet edn, 2020.
2 M. J. O'Neil, *The Merck index: an encyclopedia of chemicals, drugs and biologicals*, Whitehouse Station, N.J. Merck, 13th edn, 2001.
3 D. W. Green and R. H. Perry, in *Perry's chemical engineers' handbook*, McGraw-Hill, New York London, 8th edn, 2008.
4 R. L. Rudnick and S. Gao, Composition of the Continental Crust, in *Treatise on Geochemistry*, 2003, vol. 3–9, pp. 1–64.
5 (*a*) F. Beckers and J. Rinklebe, *Crit. Rev. Environ. Sci. Technol.*, 2017, **47**, 693; (*b*) B. Gworek, O. Bemowska-Kałabun, M. Kijeńska and J. Wrzosek-Jakubowska, *Water, Air, Soil Pollut.*, 2016, **227**, 1.
6 F. Slemr, E. G. Brunke, R. Ebinghaus and J. Kuss, *Atmos. Chem. Phys.*, 2011, **11**, 4779.
7 (*a*) N. E. Selin, *Annu. Rev. Env. Resour.*, 2009, **34**, 43; (*b*) D. Obrist, J. L. Kirk, L. Zhang, E. M. Sunderland, M. Jiskra and N. E. Selin, *Ambio*, 2018, **47**, 116; (*c*) P. A. Ariya, M. Amyot, A. Dastoor, D. Deeds, A. Feinberg, G. Kos, A. Poulain, A. Ryjkov, K. Semeniuk, M. Subir and K. Toyota, *Chem. Rev.*, 2015, **115**, 3760; (*d*) P. M. Outridge, R. P. Mason, F. Wang, S. Guerrero and L. E. Heimbürger-Boavida, *Environ. Sci. Technol.*, 2018, **52**, 11466; (*e*) C. T. Driscoll, R. P. Mason, H. M. Chan, D. J. Jacob and N. Pirrone, *Environ. Sci. Technol.*, 2013, **47**, 4967; (*f*) S. Zhu, Z. Zhang and D. Žagar, *Sci. Total Environ.*, 2018, **639**, 538; (*g*) S. J. Klapstein and N. J. O'Driscoll, *Bull. Environ. Contam. Toxicol.*, 2018, **100**, 14.
8 (*a*) D. W. Boening, *Chemosphere*, 2000, **40**, 1335; (*b*) T. W. Clarkson and L. Magos, *Crit. Rev. Toxicol.*, 2006, **36**, 609; (*c*) P. Grandjean, H. Satoh, K. Murata and K. Eto, *Environ. Health Perspect.*, 2010, **118**, 1137; (*d*) T. Syversen and P. Kaur, *J. Trace Elem. Med. Biol.*, 2012, **26**, 215; (*e*) R. Dietz, C. Sonne, N. Basu, B. Braune, T. O'Hara, R. J. Letcher, T. Scheuhammer, M. Andersen, C. Andreasen, D. Andriashek, G. Asmund, A. Aubail, H. Baagøe, E. W. Born, H. M. Chan, A. E. Derocher, P. Grandjean, K. Knott, M. Kirkegaard, A. Krey, N. Lunn, F. Messier, M. Obbard, M. T. Olsen, S. Ostertag, E. Peacock, A. Renzoni, F. F. Rigét, J. U. Skaare, G. Stern, I. Stirling, M. Taylor, T. Wiig, S. Wilson and J. Aars, *Sci. Total Environ.*, 2013, **443**, 775; (*f*) M. C. Whitney and D. A. Cristol, *Rev. Environ. Contam. Toxicol.*, 2018, **244**, 113.
9 World Health Organization - International Programme on Chemical Safety – Mercury, https://www.who.int/ipcs/assessment/public_health/mercury/en/.
10 European Commission Regulation (EC) no. 1881/2006 of 19 December 2006 setting maximum levels for certain contaminants in foodstuffs (Text with EEA relevance), https://eur-lex.Europa.eu/legal-content/EN/ALL/?uri=celex%3A32006R1881.
11 European Commission Council Directive 98/83/EC of 3 November 1998 on the quality of water intended for human consumption, https://eur-lex.Europa.eu/legal-content/EN/TXT/?uri=CELEX:31998L0083.
12 United States Environmental Protection Agency. National Primary Drinking Water Regulations. https://www.epa.gov/ground-water-and-drinking-water/national-primary-drinking-water-regulations, (22-Jun-2017).
13 United Nations - Minamata Convention on Mercury, https://treaties.un.org/doc/Treaties/2013/10/20131010%2011-16%20AM/CTC-XXVII-17.pdf.
14 United Nations Environmental Programme - Minamata Convention on Mercury, http://www.mercuryconvention.org/.
15 United Nations - Basel Convention, http://www.basel.int/TheConvention/Overview/TextoftheConvention/tabid/1275/Default.aspx.
16 United Nations - Rotterdam Convention, http://www.pic.int/TheConvention/Overview/TextoftheConvention/tabid/1048/language/en-US/Default.aspx.
17 European Commision - Tackling mercury pollution in the EU and worldwide, https://publications.Europa.eu/en/publication-detail/-/publication/7b956417-deee-11e7-9749-01aa75ed71a1/language-en.

18 K. Balasundaram and M. Sharma, *Crit. Rev. Environ. Sci. Technol.*, 2019, **49**, 1700.
19 (*a*) N. Steckling, M. Tobollik, D. Plass, C. Hornberg, B. Ericson, R. Fuller and S. Bose-O'Reilly, *Ann. Glob. Health*, 2017, **83**, 234; (*b*) T. R. Zolnikov and D. Ramirez Ortiz, *Sci. Total Environ.*, 2018, **633**, 816; (*c*) L. J. Esdaile and J. M. Chalker, *Chem. – Eur. J.*, 2018, **24**, 6905.
20 H. Gibb and K. G. O'Leary, *Environ. Health Perspect.*, 2014, **122**, 667.
21 F. Morel, A. Kraepiel and M. Amyot, *Annu. Rev. Ecol. Syst.*, 1998, **29**, 543.
22 M. M. Veiga, G. Angeloci, M. Hitch and P. C. Velasquez-Lopez, *J. Cleaner Prod.*, 2014, **64**, 535.
23 M. Amde, Y. Yin, D. Zhang and J. Liu, *Chem. Speciation Bioavailability*, 2016, **28**, 51.
24 E. W. Rice and L. Bridgewater, *Standard Methods for the Examination of Water and Wastewater*, American Public Health Association, 2012.
25 K. Leopold, M. Foulkes and P. Worsfold, *Anal. Chim. Acta*, 2010, **663**, 127.
26 Y. Gao, Z. Shi, Z. Long, P. Wu, C. Zheng and X. Hou, *Microchem. J.*, 2012, **103**, 1.
27 USEPA (United States Environmental Protection Agency), Method 1631, Revision E: Mercury in Water by Oxidation, Purge and Trap, and Cold Vapor Atomic Fluorescence Spectrometry (ed. United States Environmental Protection Agency, Washington D.C., 2002).
28 T. Rasheed, M. Bilal, F. Nabeel, H. M. N. Iqbal, C. Li and Y. Zhou, *Sci. Total Environ.*, 2018, **615**, 476.
29 E. M. Nolan and S. J. Lippard, *Chem. Rev.*, 2008, **108**, 3443.
30 (*a*) D. Dai, Z. Li, J. Yang, C. Wang, J.-R. Wu, Y. Wang, D. Zhang and Y.-W. Yang, *J. Am. Chem. Soc.*, 2019, **141**, 4756; (*b*) J. Liu, Y.-Q. Fan, S.-S. Song, G.-F. Gong, J. Wang, X.-W. Guan, H. Yao, Y.-M. Zhang, T.-B. Wei and Q. Lin, *ACS Sustainable Chem. Eng.*, 2019, **7**, 11999; (*c*) Q. Lin, Y.-Q. Fan, P.-P. Mao, L. Liu, J. Liu, Y.-M. Zhang, H. Yao and T.-B. Wei, *Chem. – Eur. J.*, 2018, **24**, 777; (*d*) X.-M. Jiang, X.-J. Huang, S.-S. Song, X.-Q. Ma, Y.-M. Zhang, H. Yao, T.-B. Wei and Q. Lin, *Polym. Chem.*, 2018, **9**, 4625; (*e*) Q. Lin, X.-M. Jiang, X.-Q. Ma, J. Liu, H. Yao, Y.-M. Zhang and T.-B. Wei, *Sens. Actuators B*, 2018, **272**, 139; (*f*) S. Yoon, A. E. Albers, A. P. Wong and C. J. Chang, *J. Am. Chem. Soc.*, 2005, **127**, 16030; (*g*) E. M. Nolan and S. J. Lippard, *J. Am. Chem. Soc.*, 2003, **125**, 14270.
31 (*a*) P. Mahato, S. Saha, P. Das, H. Agarwalla and A. Das, *RSC Adv.*, 2014, **4**, 36140; (*b*) Z. Yan, M.-F. Yuen, L. Hu, P. Sun and C.-S. Lee, *RSC Adv.*, 2014, **4**, 48373; (*c*) J. Du, J. Fan, X. Peng, P. Sun, J. Wang, H. Li and S. Sun, *Org. Lett.*, 2010, **12**, 476; (*d*) Y.-K. Yang, K.-J. Yook and J. Tae, *J. Am. Chem. Soc.*, 2005, **127**, 16760; (*e*) M.-Y. Chae and A. W. Czarnik, *J. Am. Chem. Soc.*, 1992, **114**, 9704.
32 J. H. Kim, H. J. Kim, S. H. Kim, J. H. Lee, J. H. Do, H.-J. Kim, J. H. Lee and J. S. Kim, *Tetrahedron Lett.*, 2009, **50**, 5958.
33 (*a*) W. X. Ren, S. Bhuniya, J. F. Zhang, Y. H. Lee, S. J. Lee and J. S. Kim, *Tetrahedron Lett.*, 2010, **51**, 5784; (*b*) X. Cheng, S. Li, A. Zhong, J. Qin and Z. Li, *Sens. Actuators B*, 2011, **157**, 57; (*c*) Y. Chen, C. Zhu, Z. Yang, J. Li, Y. Jiao, W. He, J. Chen and Z. Guo, *Chem. Commun.*, 2012, **48**, 5094; (*d*) A. S. Rao, D. Kim, T. Wang, K. H. Kim, S. Hwang and K. H. Ahn, *Org. Lett.*, 2012, **14**, 2598; (*e*) R. Huang, X. Zheng, C. Wang, R. Wu, S. Yan, J. Yuan, X. Weng and X. Zhou, *Chem. – Asian J.*, 2012, **7**, 915; (*f*) X. Cheng, S. Li, H. Jia, A. Zhong, C. Zhong, J. Feng, J. Qin and Z. Li, *Chem. – Eur. J.*, 2012, **18**, 1691; (*g*) X. Zhang, Y. Xu, P. Guo and X. Qian, *New J. Chem.*, 2012, **36**, 1621; (*h*) H. Dai, Y. Yan, Y. Guo, L. Fan, Z. Che and H. Xu, *Chem. – Eur. J.*, 2012, **18**, 11188; (*i*) S. Mukherjee and P. Thilagar, *Chem. Commun.*, 2013, **49**, 7292; (*j*) F. Lu, M. Yamamura and T. Nabeshima, *Dalton Trans.*, 2013, **42**, 12093; (*k*) Y. Cho, S. K. Lee, J. W. Lee, S. Ahn and S.-K. Chang, *Tetrahedron Lett.*, 2013, **54**, 5341; (*l*) S. Saha, H. Agarwalla, H. Gupta, M. Baidya, E. Suresh, S. K. Ghosh and A. Das, *Dalton Trans.*, 2013, **42**, 15097; (*m*) Y. Yan, Z. Che, X. Yu, X. Zhi, J. Wang and H. Xu, *Bioorg. Med. Chem.*, 2013, **21**, 508; (*n*) J. Jin, X. Li, J. Zhang, P. Zhao and H. Tian, *Isr. J. Chem.*, 2013, **53**, 288; (*o*) Z. Zhang, B. Zhang, X. Qian, Z. Li, Z. Xu and Y. Yang, *Anal. Chem.*, 2014, **86**, 11919; (*p*) K. Liu, Z. Xu, M. Yin, W. Yang, B. He, W. Wei and J. Shen, *J. Mater. Chem. B*, 2014, **2**, 2093; (*q*) J. Prabhu, K. Velmurugan and R. Nandhakumar, *J. Lumin.*, 2014, **145**, 733; (*r*) S. Yang, W. Yang, Q. Guo, T. Zhang, K. Wu and Y. Hu, *Tetrahedron*, 2014, **70**, 8914; (*s*) S. Madhu, S. Josimuddin and M. Ravikanth, *New J. Chem.*, 2014, **38**, 3770; (*t*) J. Zhang, J. Wang, W. Zhao and X. Dong, *Chem. Lett.*, 2015, **44**, 952; (*u*) Q.-W. Xu, C. Wang, Z.-B. Sun and C.-H. Zhao, *Org. Biomol. Chem.*, 2015, **13**, 3032; (*v*) C. Song, W. Yang, N. Zhou, R. Qian, Y. Zhang, K. Lou, R. Wang and W. Wang, *Chem. Commun.*, 2015, **51**, 4443; (*w*) Z. Ruan, C. Li, J.-R. Li, J. Qin and Z. Li, *Sci. Rep.*, 2015, **5**, 15987; (*x*) Y. Guo, J. An, H. Tang, M. Peng and F. Suzenet, *Mater. Res. Bull.*, 2015, **63**, 155; (*y*) J. Ding, H. Li, C. Wang, J. Yang, Y. Xie, Q. Peng, Q. Li and Z. Li, *ACS Appl. Mater. Interfaces*, 2015, **7**, 11369; (*z*) X. He, S. Zhu, H. Chen, Y. Wang and H. Li, *J. Lumin.*, 2016, **173**, 218.
34 (*a*) S. Bi, G. Zhang, Y. Wu, S. Wu and L. Wang, *Dyes Pigm.*, 2016, **134**, 586; (*b*) Z. Yu, Z. Tian, Z. Li, Z. Luo, Y. Li, Y. Li and J. Ren, *Sens. Actuators B*, 2016, **223**, 172; (*c*) J. Hu, Z. Hu, S. Liu, Q. Zhang, H.-W. Gao and K. Uvdal, *Sens. Actuators B*, 2016, **230**, 639; (*d*) H. Xiao, Y. Zhang, S. Li, W. Zhang, Z. Han, J. Tan, S. Zhang and J. Du, *Sens. Actuators B*, 2016, **236**, 233; (*e*) V. S. Le, J.-E. Jeong, H. T. Huynh, J. Lee and H. Y. Woo, *Sensors*, 2016, **16**, 2082; (*f*) I. J. Chang, K. S. Hwang and S.-K. Chang, *Dyes Pigm.*, 2017, **137**, 69; (*g*) H. Xiao, Y. Zhang, W. Zhang, S. Li, J. Tan and Z. Han, *Mater. Chem. Phys.*, 2017, **192**, 268; (*h*) Y. Zhou, X. He, H. Chen, Y. Wang, S. Xiao, N. Zhang, D. Li and K. Zheng, *Sens. Actuators B*, 2017, **247**, 626; (*i*) B. Gu, L. Huang, W. Su, X. Duan, H. Li and S. Yao, *Anal. Chim. Acta*, 2017, **954**, 97; (*j*) L. Tang, S. Ding, X. Zhang, K. Zhong, S. Hou and Y. Bian, *J. Photochem. Photobiol., A*, 2017, **340**, 15; (*k*) J. Ding, H. Li, Y. Xie, Q. Peng, Q. Li and

Z. Li, *Polym. Chem.*, 2017, **8**, 2221; (*l*) Y. Yang, D. Zheng, Y. Xu, Q. Liu, C. Xu, Q. Jiao and H. Zhu, *Anal. Sci.*, 2018, **34**, 1411; (*m*) Y. Shan, W. Yao, Z. Liang, L. Zhu, S. Yang and Z. Ruan, *Dyes Pigm.*, 2018, **156**, 1; (*n*) X. Cheng, S. Qu, L. Xiao, W. Li and P. He, *J. Photochem. Photobiol., A*, 2018, **364**, 503; (*o*) C. a. s. P, J. Shanmugapriya, S. Singaravadivel, G. Sivaraman and D. Chellappa, *ACS Omega*, 2018, **3**, 12341; (*p*) Z. Ruan, Y. Shan, Y. Gong, C. Wang, F. Ye, Y. Qiu, Z. Liang and Z. Li, *J. Mater. Chem. C*, 2018, **6**, 773; (*q*) Y. Gao, N. Yi, Z. Ou, Z. Li, T. Ma, H. Jia, W. Xing, G. Yang and Y. Li, *Sens. Actuators B*, 2018, **267**, 136; (*r*) L. Lan, Q. Niu and T. Li, *Anal. Chim. Acta*, 2018, **1023**, 105; (*s*) J. Xu, H. Li, Y. Chen, B. Yang, Q. Jiao, Y. Yang and H.-L. Zhu, *Anal. Methods*, 2018, **10**, 5554; (*t*) L. Wang, Y. Qu, Y. Yang, J. Cao and L. Wang, *Sens. Actuators B*, 2018, **269**, 70; (*u*) Y. Gao, T. Ma, Z. Ou, W. Cai, G. Yang, Y. Li, M. Xu and Q. Li, *Talanta*, 2018, **178**, 663; (*v*) Y. Ding, Y. Pan and Y. Han, *Ind. Eng. Chem. Res.*, 2019, **58**, 7786; (*w*) A. Sarkar, S. Chakraborty, S. Lohar, E. Ahmmed, N. C. Saha, S. K. Mandal, K. Dhara and P. Chattopadhyay, *Chem. Res. Toxicol.*, 2019, **32**, 1144; (*x*) L. Huang, Z. Yang, Z. Zhou, Y. Li, S. Tang, W. Xiao, M. Hu, C. Peng, Y. Chen, B. Gu and H. Li, *Dyes Pigm.*, 2019, **163**, 118; (*y*) L. Tang, H. Yu, K. Zhong, X. Gao and J. Li, *RSC Adv.*, 2019, **9**, 23316; (*z*) J. Ma, C. Zhang, Y. Xiao, M. Zhang, Q. Wang, W. Zheng and S. Zhang, *J. Photochem. Photobiol., A*, 2019, **378**, 142.

35 (*a*) J. Wang, Q. Niu, T. Hu, T. Li and T. Wei, *J. Photochem. Photobiol., A*, 2019, **384**, 112036; (*b*) T. Gao, X. Huang, S. Huang, J. Dong, K. Yuan, X. Feng, T. Liu, K. Yu and W. Zeng, *J. Agric. Food Chem.*, 2019, **67**, 2377; (*c*) Y. Wang, X. Hou, Z. Li, C. Liu, S. Hu, C. Li, Z. Xu and Y. Wang, *Dyes Pigm.*, 2020, **173**, 107951.

36 X. Cheng, Q. Li, C. Li, J. Qin and Z. Li, *Chem. – Eur. J.*, 2011, **17**, 7276.

37 Z. Ruan, L. Zong, Y. Song, J. Hu, J. Tu, J. Qin and Z. Li, *Sens. Actuators B*, 2016, **226**, 211.

38 (*a*) L. Chen, J. Li and L. Chen, *ACS Appl. Mater. Interfaces*, 2014, **6**, 15897; (*b*) L. Deng, Y. Li, X. Yan, J. Xiao, C. Ma, J. Zheng, S. Liu and R. Yang, *Anal. Chem.*, 2015, **87**, 2452; (*c*) X. Li, Y. Zhang, Y. Chang, B. Xue, X. Kong and W. Chen, *Biosens. Bioelectron.*, 2017, **92**, 328; (*d*) M. L. Aulsebrook, E. Watkins, M. R. Grace, B. Graham and K. L. Tuck, *ChemistrySelect*, 2018, **3**, 2088; (*e*) Z.-J. Xie, X.-Y. Bao and C.-F. Peng, *Sensors*, 2018, **18**, 2679; (*f*) Z. Chen, X. Wang, X. Cheng, W. Yang, Y. Wu and F. Fu, *Anal. Chem.*, 2018, **90**, 5489; (*g*) P. Donati, M. Moglianetti, M. Veronesi, M. Prato, G. Tatulli, T. Bandiera and P. P. Pompa, *Angew. Chem., Int. Ed.*, 2019, **58**, 10285.

39 R. S. H. Liu, *J. Chem. Educ.*, 2002, **79**, 183.

40 R. S. H. Liu and A. E. Asato, *J. Photochem. Photobiol., C*, 2003, **4**, 179.

41 (*a*) H. Xin, J. Li, X. Yang and X. Gao, *J. Org. Chem.*, 2020, **85**, 70; (*b*) D. Lichosyt, S. Wasiłek, P. Dydio and J. Jurczak, *Chem. – Eur. J.*, 2018, **24**, 11683; (*c*) H. Fang, Y. Gan, S. Wang and T. Tao, *Inorg. Chem. Commun.*, 2018, **95**, 17; (*d*) S. Wakabayashi, M. Uchida, R. Tanaka, Y. Habata and M. Shimizu, *Asian J. Org. Chem.*, 2013, **2**, 786.

42 (*a*) S. Wakabayashi, R. Uriu, T. Asakura, C. Akamatsu and Y. Sugihara, *Heterocycles*, 2008, **75**, 383; (*b*) S. Wakabayashi, R. Yamaoka, E. Matsumoto, M. Nishiguchi, M. Ishiura, M. Tsuji and M. Shimizu, *Heterocycles*, 2012, **85**, 2251; (*c*) S. Wakabayashi, Y. Kato, K. Mochizuki, R. Suzuki, M. Matsumoto, Y. Sugihara and M. Shimizu, *J. Org. Chem.*, 2007, **72**, 744.

43 (*a*) A. C. Razus, L. Birzan, M. Cristea, V. Tecuceanu, A. Hanganu and C. Enache, *J. Heterocycl. Chem.*, 2011, **48**, 1019; (*b*) L. Birzan, M. Cristea, C. C. Draghici, V. Tecuceanu, A. Hanganu, E.-M. Ungureanu and A. C. Razus, *Tetrahedron*, 2017, **73**, 2488.

44 (*a*) G.-O. Buica, I.-G. Lazar, L. Birzan, C. Lete, M. Prodana, M. Enachescu, V. Tecuceanu, A. B. Stoian and E.-M. Ungureanu, *Electrochim. Acta*, 2018, **263**, 382; (*b*) G.-O. Buica, A. A. Ivanov, I.-G. Lazar, G.-L. Tatu (Arnold), C. Omocea, L. Birzan and E.-M. Ungureanu, *J. Electroanal. Chem.*, 2019, **849**, 113351.

45 K. Kubo, A. Mori, T. Nishimura and N. Kato, *Heterocycles*, 2008, **76**, 209.

46 (*a*) L. C. Murfin, K. Chiang, G. T. Williams, C. L. Lyall, A. T. A. Jenkins, J. Wenk, T. D. James and S. E. Lewis, *Front. Chem.*, 2020, DOI: 10.3389/fchem.2020.00010; (*b*) L. C. Murfin, C. M. López-Alled, A. C. Sedgwick, J. Wenk, T. D. James and S. E. Lewis, *Front. Chem. Sci. Eng.*, 2020, **14**, 90–96; (*c*) S. J. Webster, C. M. López-Alled, X. Liang, C. L. McMullin, G. Kociok-Köhn, C. L. Lyall, T. D. James, J. Wenk, P. J. Cameron and S. E. Lewis, *New J. Chem.*, 2019, **43**, 992; (*d*) L. C. Murfin, M. Weber, S. J. Park, W. T. Kim, C. M. López-Alled, C. L. McMullin, F. Pradaux-Caggiano, C. L. Lyall, G. Kociok-Köhn, J. Wenk, S. D. Bull, J. Yoon, H. M. Kim, T. D. James and S. E. Lewis, *J. Am. Chem. Soc.*, 2019, **141**, 19389–19396; (*e*) P. Cowper, A. Pockett, G. Kociok-Köhn, P. J. Cameron and S. E. Lewis, *Tetrahedron*, 2018, **74**, 2775; (*f*) C. M. López-Alled, A. Sanchez-Fernandez, K. J. Edler, A. C. Sedgwick, S. D. Bull, C. L. McMullin, G. Kociok-Köhn, T. D. James, J. Wenk and S. E. Lewis, *Chem. Commun.*, 2017, **53**, 12580; (*g*) P. Cowper, Y. Jin, M. D. Turton, G. Kociok-Köhn and S. E. Lewis, *Angew. Chem., Int. Ed.*, 2016, **55**, 2564.

47 W. Treibs, H. J. Neupert and J. Hiebsch, *Chem. Ber.*, 1959, **92**, 141.

48 (*a*) A. B. Smith III, W. Zhu, S. Shirakami, C. Sfouggatakis, V. A. Doughty, C. S. Bennett and Y. Sakamoto, *Org. Lett.*, 2003, **5**, 761; (*b*) T. E. Burghardt, *J. Sulfur Chem.*, 2005, **26**, 411.

49 J. Zembrzuska, I. Budnik and Z. Lukaszewski, *Sci. Total Environ.*, 2016, **557–558**, 612.